ADVANCED HEALTHCARE MATERIALS
www.advhealthmat.de

Autoantigen-Dexamethasone Conjugate-Loaded Liposomes Halt Arthritis Development in Mice

Naomi Benne, Daniëlle ter Braake, Deja Porenta, Chun Yin Jerry Lau, Enrico Mastrobattista, and Femke Broere*

There is no curative treatment for chronic auto-inflammatory diseases including rheumatoid arthritis, and current treatments can induce off-target side effects due to systemic immune suppression. This work has previously shown that dexamethasone-pulsed tolerogenic dendritic cells loaded with the arthritis-specific antigen human proteoglycan can suppress arthritis development in a proteoglycan-induced arthritis mouse model. To circumvent ex vivo dendritic cell culture, and enhance antigen-specific effects, drug delivery vehicles, such as liposomes, provide an interesting approach. Here, this work uses anionic 1,2-distearoyl-sn-glycero-3-phosphoglycerol liposomes with enhanced loading of human proteoglycan-dexamethasone conjugates by cationic lysine tetramer addition. Antigen-pulsed tolerogenic dendritic cells induced by liposomal dexamethasone in vitro enhanced antigen-specific regulatory T cells to a similar extent as dexamethasone-induced tolerogenic dendritic cells. In an inflammatory adoptive transfer model, mice injected with antigen-dexamethasone liposomes have significantly higher antigen-specific type 1 regulatory T cells than mice injected with antigen only. The liposomes significantly inhibit the progression of arthritis compared to controls in preventative and therapeutic proteoglycan-induced arthritis mouse models. This coincides with systemic tolerance induction and an increase in *IL10* expression in the paws of mice. In conclusion, a single administration of autoantigen and dexamethasone-loaded liposomes seems to be a promising antigen-specific treatment strategy for arthritis in mice.

1. Introduction

Rheumatoid arthritis (RA) is a common auto-immune disease with a worldwide prevalence of 0.46%.[1] RA is characterized by an influx of pro-inflammatory immune cells into the synovium, resulting in synovial lining hyperplasia and the destruction of bone and articular cartilage,[2] leading to pain and disability. No curative treatments are currently available for RA, and available treatment modalities such as disease-modifying antirheumatic drugs (DMARDs), non-steroidal anti-inflammatory agents (NSAIDS), and corticosteroids[3,4] often bring about off-target side effects as they are not antigen-specific and generally immunosuppressive. This leaves patients more susceptible to developing other complications, such as viral infections.[5] Recently, there have been developments in the field of antigen-specific immunotherapy for autoimmune diseases, specifically focusing on tolerogenic dendritic cells (tolDCs).[6] These tolDCs are a specialized subset of DCs that can induce $CD4^+CD25^+FoxP3^+$ regulatory T cells (Tregs) and $CD49^+LAG\text{-}3^+$ type 1 regulatory T cells (Tr1) and can inhibit the

N. Benne, D. ter Braake, D. Porenta, F. Broere
Department of Infectious Diseases and Immunology
Faculty of Veterinary Medicine
Utrecht University
Utrecht 3584 CL, The Netherlands
E-mail: n.benne@uu.nl

The ORCID identification number(s) for the author(s) of this article can be found under https://doi.org/10.1002/adhm.202304238

DOI: 10.1002/adhm.202304238

D. Porenta, C. Y. J. Lau, E. Mastrobattista
Utrecht Institute for Pharmaceutical Sciences
Department of Pharmaceutics
Faculty of Science
Utrecht University
Utrecht 3584 CG, The Netherlands

C. Y. J. Lau
Department of Materials Engineering
Graduate School of Engineering
The University of Tokyo
7-3-1 Hongo, Bunkyo-ku, Tokyo 113-8656, Japan

proliferation of effector $CD4^+$ T cells (Teff), such as $Tbet^+$ T helper 1 (Th1), or $ROR\gamma T^+$ Th17 cells.[7] It has been shown that this skewing toward Tregs/Tr1 and away from other Th subsets is beneficial for the treatment of autoimmunity, including RA.[8] TolDCs are generally characterized by a semi-mature $CD11c^+MHCII^+CD40^{lo}CD86^{lo}$ phenotype, limiting their co-stimulatory abilities. Simultaneously a shift in cytokine production from pro-inflammatory (e.g., IL-12, TNFα) to anti-inflammatory (e.g., IL-10, TGF-β) occurs in these cells. The lack of co-stimulation results in effector T cell anergy,[9–11] whilst also promoting Treg differentiation.[9,12–15] TolDCs can be induced through the addition of immunomodulators, such as dexamethasone (Dex),[16] vitamin D3,[17] or retinoic acid.[18] A great advantage of using tolDCs for immunotherapy is the ability to load them with disease-relevant antigens, allowing for antigen-specific tolerance induction. This results in a suppressive response specifically toward the disease-causing antigen while avoiding systemic immune suppression that would result from suppressive responses toward other antigens.

At present, differentially generated tolDCs are tested in clinical trials worldwide to assess their efficacy and safety (*NCT02903537*,[19] *NCT01352858*,[20] *NCT05251870*), and results so far are promising.[21,22] However, just like other cell-based therapies, tolDC therapy is restricted to specialized cell culture and medical facilities, which makes this therapy costly and not widely accessible to patients. Therefore, there is a clear need for a new treatment strategy that allows for easy, low-cost production whilst simultaneously facilitating the beneficial effects also observed in current cell-based treatment options. The use of nanoparticles, such as liposomes, which encapsulate both an immunomodulator and an antigen is a promising strategy to circumvent these limitations.[23–26]

Liposomes are drug-delivery vehicles that consist of one or more lipid bilayers that form around an aqueous core,[27,28] allowing for the encapsulation of cargo with different physiochemical properties.[23] Depending on the properties of these liposomes, they can modulate immune responses to induce the desired T cell responses. We have previously shown that anionic 1,2-distearoyl-sn-glycero-3-phosphoglycerol (DSPG)-containing liposomes can induce strong antigen-specific Treg responses.[29] These liposomes facilitate the efficient uptake of antigens by antigen-presenting cells (APCs), such as DCs.[18] When loaded with an atherosclerosis-specific antigen, these liposomes have been shown to reduce disease progression in an atherosclerotic mouse model,[29] highlighting their therapeutic potential. Nanoparticles encapsulating both immunomodulators and disease-relevant antigens are potent tolerance inducers.[30,31] Therefore, we aimed to enhance the tolerogenic effect of the DSPG-liposomes by including an immunomodulator, such as Dex. Dex is a potent inducer of tolerance in DCs. Upon Dex interaction with the glucocorticoid receptor (GR), gene transcription of IL-10 is increased,[32,33] and transcription of pro-inflammatory genes, such as IL-12, is inhibited.[34] Dex has been described as an effective treatment option for a plethora of inflammatory diseases, including rheumatoid arthritis.[11] Dex is poorly soluble in water (logP 1.68), which does lead to beneficial transmembrane transport and in vivo bioavailability, but limits encapsulation in liposomes containing high T_m lipids and cholesterol.[35,36] Additionally, when Dex is administered systemically, it can result in severe side effects owing to non-specific immune suppression, especially after long-term use.[37]

Therefore, to minimize the risk of off-target effects and increase encapsulation in liposomes, Dex was linked to the antigen epitope via a biodegradable spacer to form a single entity for liposomal encapsulation. Furthermore, a lysine tetramer (K4) was added adjacent to the Dex, to provide a cationic moiety for electrostatic complexation with anionic DSPG, thereby facilitating liposomal loading. This study aimed to induce antigen-specific immune tolerance to an RA-causing antigen, thereby mitigating the progression of RA in preventative and curative mouse models for RA. We hypothesized that DSPG-liposomes loaded with autoantigen-human proteoglycan (hPG)-Dex conjugate can improve the induction of antigen-specific immune suppression.

We show that the antigen-Dex conjugates can be efficiently encapsulated in liposomes. hPG_{K4}-Dex liposomes induce IDO, TLR2, and IL-10 in DCs, which in turn can increase levels of antigen-specific Tr1 cells in vitro and in vivo. Subsequently, these hPG_{K4}-Dex liposomes can protect against arthritis development in a murine model for PGIA and even halt the progression of established disease. At the end of the therapeutic arthritis study, we observed a reduction of hPG-specific IgG1 autoantibodies and splenic $CD86^+CD11c^+$ cells, and we noticed an increase in splenic $CD25^+Foxp3^+$ and PD-1^+ $CD4^+$ T cells in hPG_{K4}-Dex liposome treated mice compared to controls. In the paws of these mice, we measured high IL-10 which indicates local immune protection. This shows that hPG_{K4}-Dex liposomes are a promising treatment strategy for RA in mice.

Table 1. Physicochemical characterization of Dex-loaded liposomes. The Z_{ave} size, polydispersity index (PDI), ζ-potential and % antigen encapsulation in the liposomes.

Cargo	Z_{ave} [nm][a)]	PDI	Z-potential [mV]	% LE[b)]
Empty	191.2 ± 6.3	0.11 ± 0.03	−54.1 ± 3.6	–
hPG	187.6 ± 14.1	0.06 ± 0.03	−47.7 ± 2.1	10.4 ± 6.6
hPG_{K4}	199.4 ± 6.2	0.06 ± 0.02	−51.3 ± 3.8	45.9 ± 11.4
hPG_{K4}-Dex	195.7 ± 21.4	0.08 ± 0.01	−54.9 ± 5.4	46.5 ± 10.8
OVA_{323K4}-Dex	192.3 ± 17.9	0.07 ± 0.03	−52.0 ± 2.9	49.6 ± 11.8

[a)] Z-average diameter (Z_{ave}), mean ± SD, $n = 3$; [b)] %LE (loading $_{efficiency}$) was calculated as the total amount of peptide before extrusion/total amount of peptide after purification * 100%.

2. Results

2.1. Dex, Free or Encapsulated in Liposomes, Induces a Tolerogenic Phenotype in DCs In Vitro

The arthritis-relevant MHC-II autoantigen hPG and the ovalbumin-derived MHC-II-restricted $OVA_{323–339}$ antigen were extended with a lysine tetramer to couple to Dex (forming hPG_{K4}-Dex and OVA_{323K4}-Dex, respectively). The antigens were encapsulated into anionic DSPG liposomes. The liposomes, with or without antigen loading, were below 200 nm in size and had a negative surface charge. The LE of the antigen-Dex complexes was between 46.5 and 49.6% (see **Table 1**). The addition of the lysine tetramer enhanced the LE of the antigen from 10.4%, and of Dex from 0.02% (Figure S1, Supporting Information).

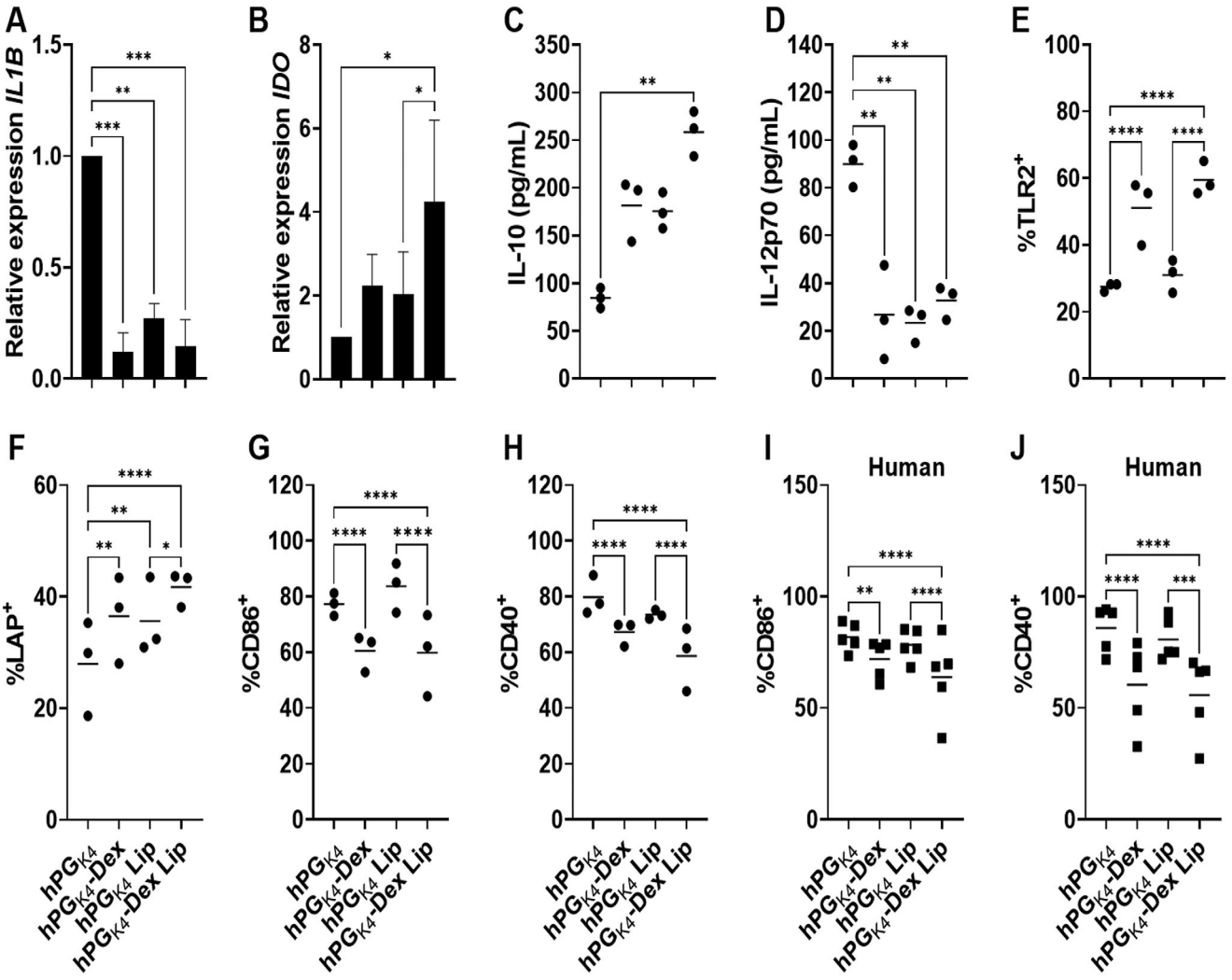

Figure 1. hPG_{K4}-Dex, free or encapsulated in liposomes, induces a tolerogenic phenotype in Balb/cAnNCrl BMDCs and human moDCs. Immature BMDCs cultured from the bone marrow of Balb/cAnNCrl mice or human moDCs cultured from $CD14^+$ cells isolated from buffy coats of healthy donors were stimulated overnight with hPG_{K4} + LPS, hPG_{K4}-Dex + LPS, hPG_{K4} Liposomes (Lip) + LPS, or hPG_{K4}-Dex Lip + LPS. Relative expression of A) *IL1B* and B) *IDO*, normalized based on *HPRT* expression and relative to the hPG_{K4} group, measured by qPCR. C) IL-10 and D) IL-12p70 concentration was measured in supernatants of BMDCs (pg mL^{-1}) using ELISA. E) $\%TLR2^+$, F) $\%LAP^+$, G) $\%CD86^+$, and H) $\%CD40^+$ in BMDCs, and I) $\%CD86^+$ and J) $\%CD40^+$ in moDCs as measured by flow cytometry in the live $CD11c^+$ population. Means (+ SD), ** $p < 0.01$, *** $p < 0.001$, **** $p < 0.0001$ as determined by two-way ANOVA and Tukey's multiple comparisons test.

To evaluate the tolerance induction by free or encapsulated Dex, immature BMDCs were stimulated overnight with LPS and either free or encapsulated hPG_{K4} and hPG_{K4}-Dex. Gene expression of *IL1B* was greatly reduced when BMDCs were incubated with hPG_{K4}-Dex, hPG_{K4} liposomes, or hPG_{K4}-Dex encapsulated in liposomes compared to the hPG_{K4} control (**Figure 1A**). Interestingly encapsulation in liposomes seems to enhance the tolerogenic capacity of hPG_{K4}-Dex, as evidenced by the increased gene expression of IDO (Figure 1B), and the release of IL-10 (Figure 1C). Secretion of IL-12p70 was also reduced in all groups compared to the positive control (Figure 1D). Dex, free or encapsulated, increased the expression of Toll-like receptor 2 (TLR2) (Figure 1E and Figure S2A,B, Supporting Information), and latency-associated protein (LAP, the membrane-bound form of TGF-β) (Figure 1F and Figure S2C, Supporting Information). This coincided with a reduction in the expression of costimulatory molecules CD86 and CD40 in BMDCs and moDCs (Figure 1G and Figure S2D, Supporting Information and Figure 1H and Figure S2E, Supporting Information and Figure 1I, and Figure 1J). We also observed that Dex liposomes had more efficient uptake by BMDCs as compared to Dex-free liposomes, possibly due to an increase in the phagocytic receptor MerTK (Figure S3, Supporting Information).

2.2. Dex-Linked hPG Induces Antigen-Specific Tregs In Vitro and In Vivo

As shown above, hPG_{K4}-Dex liposomes can induce phenotypical tolDCs with a cytokine secretion and gene expression profile

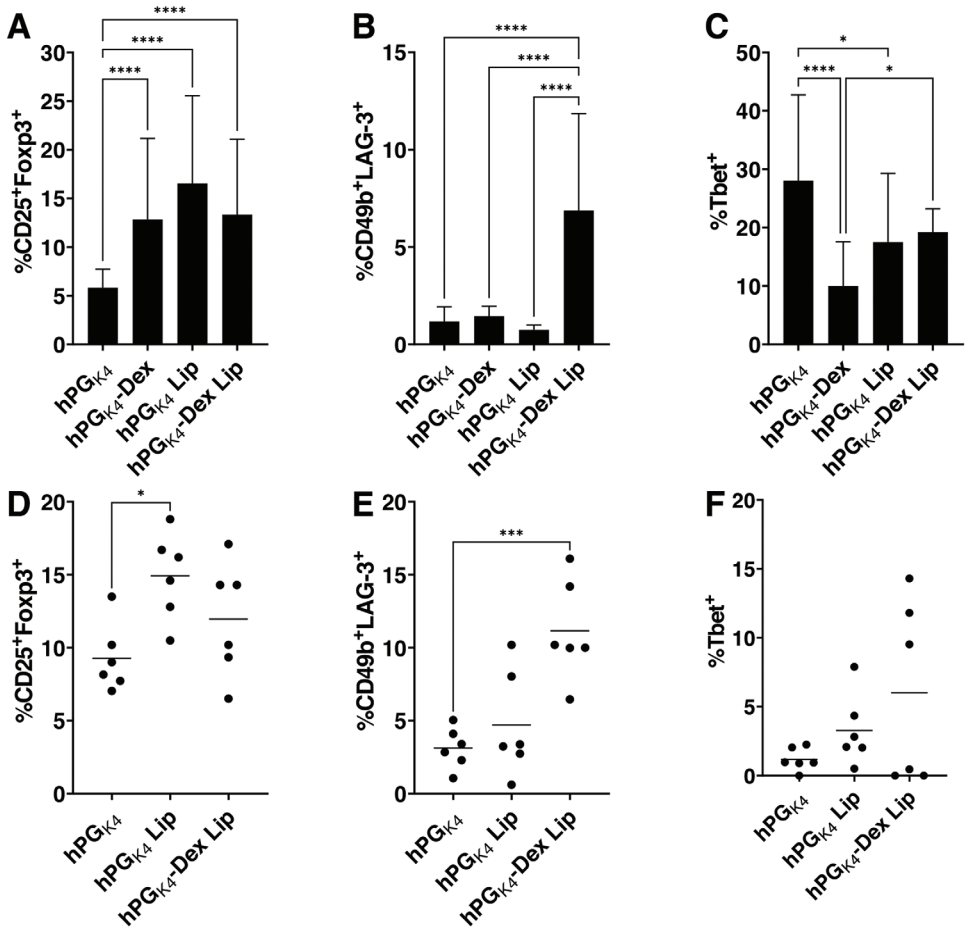

Figure 2. Antigen-specific T cell skewing by hPG_{K4}-Dex liposomes in vitro and in vivo. Immature BMDCs cultured from the bone marrow of Balb/cAnNCrl mice were stimulated overnight with hPG_{K4} + LPS, hPG_{K4}-Dex + LPS, hPG_{K4} Liposomes (Lip) + LPS, or hPGDex Lip + LPS. Cells were washed and CFSE-labelled $CD4^+$ T cells from hPG-TCR mice were co-incubated for 3 days with the BMDCs. A) $\%CD25^+Foxp3^+$ B) $\%CD49b^+LAG\text{-}3^+$, and C) $\%Tbet^+$ cells of $CFSE^-CD4^+$ T cells, measured by flow cytometry, $n = 3$. Thy1.1$^-$ Balb/cAnNCrl mice were injected intramuscularly with hPG protein, followed intravenously with 500 000 $Thy1.1^+$ hPG-TCR $CD4^+$ T cells. This induces hPG-specific inflammatory responses and an expansion of the hPG-TCR $CD4^+$ T cells. 1 day later, mice were injected intravenously with 1 nmol hPG_{K4} or 1 nmol hPG_{K4}-Dex encapsulated in liposomes. 3 days later, mice were sacrificed, and spleens were isolated for flow cytometry. D) $\%CD25^+Foxp3^+$ E) $\%CD49b^+LAG\text{-}3^+$, and F) $\%Tbet^+$ cells of $Thy1.1^+CD4^+$ T cells, $n = 6$. Means (+ SD), * $p < 0.05$, ** $p < 0.01$, *** $p < 0.001$, **** $p < 0.0001$, as determined by one-way ANOVA and Tukey's multiple comparisons test (in vitro) or Bonferroni's multiple comparisons test (in vivo).

that is hypothesized to promote tolerance in T cells. Next, the effect of these tolDCs on antigen-specific T cells was assessed in vitro and in vivo. Both free and encapsulated hPG_{K4}-Dex pulsed DCs increased antigen-specific $CD25^+Foxp3^+$ Tregs. hPG_{K4} liposomes without Dex also increase Tregs (**Figure 2A**). Only encapsulated Dex increased $CD49b^+LAG\text{-}3^+$ Tr1 cells (Figure 2B). Both free and encapsulated Dex decreased antigen-specific T-bet$^+$ Th1 cells, although free Dex was more potent than encapsulated Dex. Dex-free liposomes also reduced Th1 cells (Figure 2C). In a naïve adoptive transfer model, OVA_{323K4}-Dex liposomes were able to expand antigen-specific $CD25^+Foxp3^+$ Tregs (Figure S4, Supporting Information). In an inflammatory in vivo adoptive transfer model, intravenous injection of hPG_{K4} liposomes induced antigen-specific $CD25^+Foxp3^+$ Tregs, while hPG_{K4}-Dex liposomes could not skew the $CD4^+$ T cell response toward $CD25^+Foxp3^+$ Tregs in the pro-inflammatory environment (Figure 2D). The hPG_{K4}-Dex liposomes did greatly enhance antigen-specific $CD49b^+LAG\text{-}3^+$ Tr1 cells (Figure 2E) compared to free antigen. Tbet$^+$ Th1 cell levels also seemed enhanced in the mice receiving hPG_{K4}-Dex liposomes, albeit non-specifically (Figure 2F). This shows that hPG_{K4}-Dex liposomes can induce strong Tr1 responses, even in an inflammatory environment, which is hypothesized to be necessary for suppressing the responses in an arthritis model.

2.3. Arthritis Development in Mice is Inhibited by hPG_{K4}-Dex Liposomes

Based on the results, we hypothesized that the hPG_{K4}-Dex liposomes would give the best protection in a model of arthritis. To assess the pre-clinical efficacy of the hPG_{K4}-Dex liposomes we employed the PGIA mouse model. First, we performed a preventative study, whereby mice were injected intravenously with

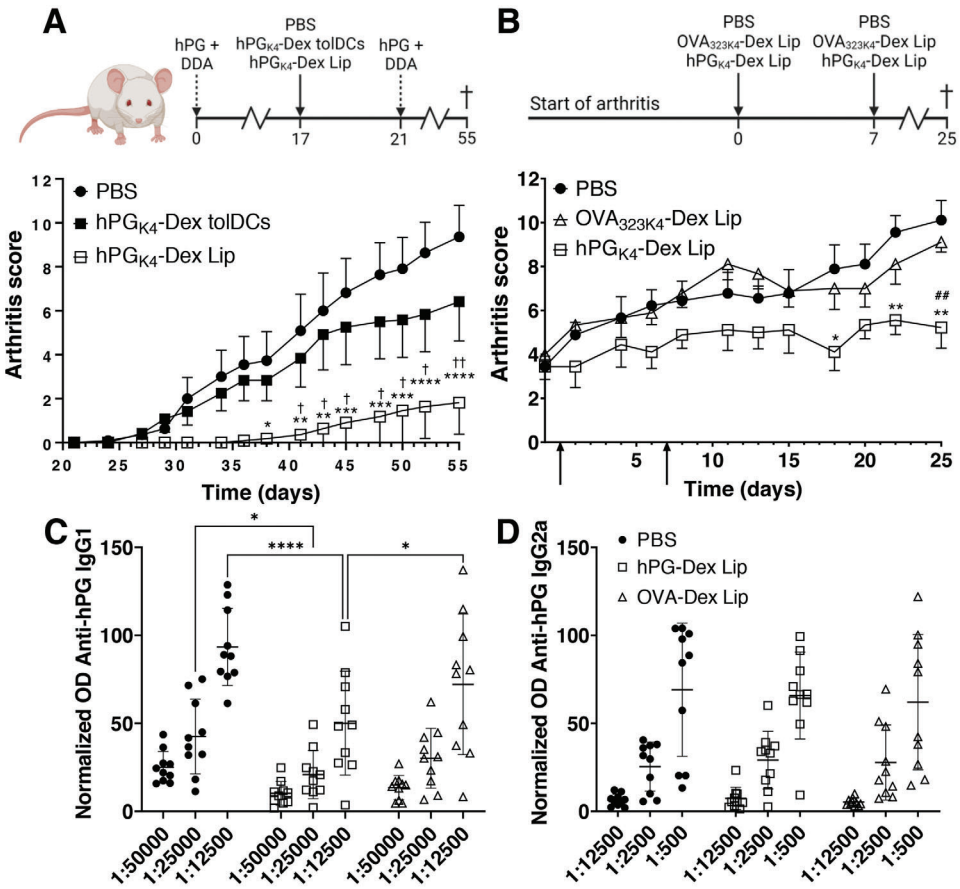

Figure 3. hPG_{K4}-Dex Liposomes inhibit the development of arthritis in mice. Female Balb/cAnNCrl mice were injected i.p. on days 0 and 21 with a mixture of 2 mg DDA and 250 µg human proteoglycan to induce arthritis. A) In the preventative model mice were treated on day 17 via intravenous injection of PBS, hPG_{K4}-Dex tolDCs (20 nmol hPG_{K4}-Dex), or hPG_{K4}-Dex liposomes (2 nmol hPG_{K4}-Dex). B) In the curative model, mice were enrolled after arthritis was established based on visual scoring and treated on days 0 and 7 after arthritis induction via intravenous injection of PBS, hPG_{K4}-Dex liposomes (2 nmol hPG_{K4}-Dex), or OVA_{323K4}-Dex liposomes (2 nmol OVA_{323K4}-Dex). Means ± SEM, * $p < 0.05$, ** $p < 0.01$, *** $p < 0.001$, **** $p < 0.0001$ compared to PBS group, and † $p < 0.05$, †† $p < 0.01$ compared to hPG_{K4}-Dex tolDCs, and ## $p < 0.01$ compared to OVA_{323K4}-Dex liposomes as determined by two-way ANOVA and Bonferroni's multiple comparisons test. C) Anti-hPG IgG1 and D) IgG2a antibodies were measured in the serum of mice 25 days after the first injection of the treatment by ELISA. OD values per plate were normalized based on a calibration curve. The serum dilutions are shown on the x-axis. Means + SD, * $p < 0.05$, **** $p < 0.0001$, as determined by one-way ANOVA and Bonferroni's multiple comparisons tests.

PBS, 1×10^6 hPG_{K4}-Dex tolDCs (equivalent to 20 nmol of hPG_{K4}-Dex), or hPG_{K4}-Dex liposomes (2 nmol of hPG_{K4}-Dex) before they had developed arthritis (**Figure 3A**). Mice that were treated with hPG_{K4}-Dex liposomes developed significantly less arthritis compared to the PBS and even the hPG_{K4}-Dex-pulsed tolDC-treated mice, as shown by a lower arthritis score (Figure 3A). Furthermore, while 100% of mice in the PBS group had developed arthritis (score of 2 or higher), 75% and 27% of mice in the hPG_{K4}-Dex-pulsed tolDC and hPG_{K4}-Dex liposomes groups, respectively, developed arthritis (Table S1, Supporting Information). Next, we wanted to see whether the hPG_{K4}-Dex liposomes could halt the progression of arthritis in mice that had ongoing inflammation (Figure 3B). In this model, we observed that they could indeed stabilize arthritis in mice, compared to PBS and compared to OVA_{323K4}-Dex liposomes (Figure 3B). 100% of mice in the PBS and OVA_{323K4}-Dex liposomes groups had increased arthritis scores compared to the day of the first injection, while 33% of mice treated with hPG_{K4}-Dex liposomes had a lower score at the end of the experiment compared to the start (Table S1, Supporting Information). Anti-hPG IgG1 and IgG2a were measured in the serum of mice after sacrifice. Mice that received hPG_{K4}-Dex liposomes overall had lower amounts of anti-hPG IgG1 compared to the other groups, but not IgG2a (Figure 3C,D).

Further analysis of the spleens of mice sacrificed on day 25 after the first injection of liposomes or control revealed that, in the mice that received the hPG_{K4}-Dex liposomes, the $\%CD11c^+CD86^+$ DCs were reduced compared to the other groups (**Figure 4A**), while PD-L1 was unchanged (Figure 4B). This coincided with an increase in $CD25^+Foxp3^+$ and $PD\text{-}1^+$ regulatory T cells (Figure 4C,D) within the $CD4^+$ T cell population (Figure S5, Supporting Information). $ROR\gamma T^+$, and $Tbet^+$ populations were unchanged (Figure 4E,F). Interestingly, in the paws of mice, we observed a non-significant reduction in *MPO* and *IL1B* (Figure 4G,H) while the expression of *IL10* was enhanced (Figure 4I).

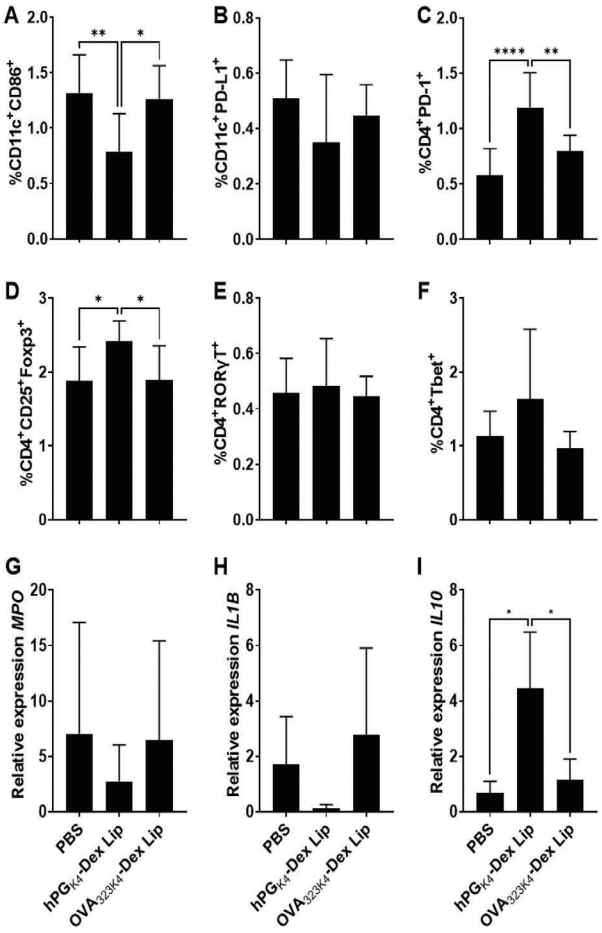

Figure 4. hPG$_{K4}$-Dex liposomes enhance tolerogenic responses in arthritic mice. Female Balb/cAnNCrl mice were injected i.p. on days 0 and 21 with a mixture of 2 mg DDA and 250 µg human proteoglycan to induce arthritis. Mice were enrolled after arthritis was established and treated on days 0 and 7 via intravenous injection of PBS, hPG$_{K4}$-Dex liposomes (2 nmol hPG$_{K4}$-Dex), or OVA$_{323K4}$-Dex liposomes (2 nmol OVA$_{323K4}$-Dex). Mice were sacrificed on day 25 and organs were isolated for analysis. A) CD11c$^+$CD86$^+$ DCs, B) CD11c$^+$PD-L1$^+$ DCs, C) CD4$^+$PD-1$^+$ T cells, D) CD4$^+$CD25$^+$Foxp3$^+$ Tregs, E) CD4$^+$RORγT$^+$ Th17, and F) CD4$^+$Tbet$^+$ Th1 cells, % of all live cells in the spleen, measured by flow cytometry. G) *MPO*, H) *IL1B*, and I) *IL10* expression in the paws of mice, normalized based on *HPRT* expression using the Pfaffl method, measured by qPCR. Means + SD, * $p < 0.05$, ** $p < 0.01$, **** $p < 0.0001$ as determined by one-way ANOVA and Bonferroni's multiple comparisons test.

3. Discussion

Restoring immune tolerance is essential for the treatment of autoimmune and chronic inflammatory diseases. Current clinical trials are making use of DCs pulsed with immunomodulators and disease-relevant antigens to achieve this.[19–22] Despite encouraging results, the production of these tolDCs requires specialized research centers and is costly, making them less accessible to the large groups of patients that need treatment. Accordingly, there's a need for a strategy that overcomes these limitations. Nanoparticles, including liposomes, are promising drug-delivery vehicles that can surpass the need for ex vivo culturing of tolDCs.[23–26] Here, we prepared anionic DSPG-containing liposomes for the delivery of novel antigen-Dex conjugates to induce antigen-specific immune tolerance in vitro, in vivo, and in a pre-clinical model for RA. Dex was chosen because of its potent immune-suppressing properties and proven ability to induce tolDCs.[34–36] However, it is known that Dex can induce side effects, especially at high doses.[37] Therefore, we coupled Dex to our antigens of interest with the aim of preventing the uptake of Dex by APCs in a non-antigen-specific context, thereby minimizing non-antigen-specific effects. In addition, we hypothesized that the liposomes facilitated more efficient uptake of antigen-Dex conjugates by APCs than free antigen-Dex conjugates, allowing us to greatly reduce the required dose, further minimizing side effects. To optimize the liposomal preparation, we reasoned that adding lysine tetramer to antigen-Dex conjugates could enable electrostatic complexation with DSPG, which resulted in a marked enhancement of LE (Figure S1, Supporting Information).

BMDCs and moDCs exhibit a tolerogenic phenotype upon stimulation with free hPG$_{K4}$-Dex (Figure 1). This is in line with previous research showing the effect of Dex on DCs, using similar assays and Dex concentrations.[43,44] This indicates that the linking of Dex to an antigen does not hinder the functionality of Dex. Encapsulation of hPG$_{K4}$-Dex into liposomes crucially does not impede the immunomodulatory effects of Dex (Figures 1 and 2). On the contrary, stimulation of DCs with hPG$_{K4}$-Dex liposomes increased gene expression of *IDO* (Figure 1B), the release of IL-10 (Figure 1C), and protein expression of LAP (Figure 1F) compared to free hPG$_{K4}$-Dex. Dex is a GR ligand that must cross the host cell membrane and bind to GRs present in the cell cytoplasm in order to exert its effects.[45,46] Accordingly, enhanced intracellular delivery of Dex by liposomes could increase interactions with GRs, possibly explaining the enhanced effects observed after hPG$_{K4}$-Dex liposome treatment. The DSPG-liposomes themselves have tolerogenic properties, as we have shown before,[29] but the addition of Dex enhanced some of these effects (Figure 1). Dex stimulates uptake of liposomes, possibly due to an increase in the phagocytic receptor MerTK (Figure S3, Supporting Information). This increased uptake of the inherently tolerogenic liposomes, together with the tolerogenic properties of Dex, could explain why the Dex-containing liposomes show a more favorable tolDC phenotype.

Our studies using TCR-specific transgenic CD4$^+$ T cells indicate that the coupling of Dex to an antigen via the lysine tetramer does not prevent MHC presentation by DCs and subsequent TCR recognition by antigen-specific T cells as we observe potent T cell responses. The most striking result is that hPG$_{K4}$-Dex liposome-treated BMDCs increase CD49b$^+$LAG-3$^+$ Tr1 numbers in in vitro co-culture experiments (Figure 2B), while free Dex and liposomes without Dex do not induce Tr1 cells. In a naïve adoptive transfer model, OVA$_{323K4}$-Dex liposomes were able to expand antigen-specific CD25$^+$Foxp3$^+$ Tregs to the same extent as free OVA$_{323K4}$-Dex (Figure S4, Supporting Information), albeit at a much lower dose (1 nmol versus 85 nmol). Kim et al. reported that poly (lactic-*co*-glycolic acid) (PLGA)-nanoparticles co-encapsulating OVA and Dex, using a comparable dose of Dex (administered orally) as described in this paper, resulted in antigen-specific Treg induction compared to nanoparticles with OVA alone in an adoptive transfer model.[30] In an inflammatory adoptive transfer model, hPG$_{K4}$-Dex liposome induced antigen-specific CD49b$^+$LAG-3$^+$

Tr1 cells (Figure 3E). Antigen-specific $CD25^+Foxp3^+$ Tregs were increased in the inflammatory adoptive transfer model in mice that received hPG_{K4} liposomes, but not hPG_{K4}-Dex liposomes (Figure 3D). This indicates that, in an inflammatory environment, the hPG_{K4}-Dex liposomes lose the ability to induce or maintain antigen-specific Tregs, while they can still enhance Tr1 cells. This difference between the skewing of T cell subsets between Dex-free and Dex-liposomes could be explained by the fact that the Dex liposomes inhibited costimulatory molecules in DCs,[47] and increased IL-10, LAP,[48] *IDO*,[49,50] and TLR2[51,52] compared to Dex-free liposomes (Figure 1). Furthermore, Dex has previously been shown to upregulate glucocorticoid-induced tumor necrosis factor-receptor family-related gene (GITR) expression in a variety of T cells,[53] and the interaction between GITR and its ligand (GITRL) has been previously shown to be responsible for an increase in Tr1 cells.[54] However, it should be stated that the consequences of GITR activation are complex and can be dependent on the activation state of T cells and the host environment.

Since the hPG_{K4}-Dex liposomes induced potent Tr1 responses, and these responses are important for protection against arthritis,[52] we decided to test these liposomes in a murine PGIA disease model for arthritis. hPG_{K4}-Dex liposomes significantly reduced arthritis development compared to mice that received hPG_{K4}-Dex tolDCs or PBS (Figure 3A). It should be stated that antigen-loaded dexamethasone-induced tolDCs are a potent therapy against rheumatoid arthritis, and the lack of effect in the current study is likely due to the suboptimal dose of hPG_{K4}-Dex.[11,55] More importantly, the liposomes could prevent the further progression of arthritis in mice that had established diseases (Figure 3B). The lack of arthritis development in mice that received hPG_{K4}-Dex liposomes is more pronounced than in previous research using arthritis-related agent-pulsed tolDC therapy in a mouse model.[7,11] It was previously shown in an experimental autoimmune encephalomyelitis (EAE) model that co-encapsulation of MOG with Dex in Dextran nanoparticles was essential to treat disease; MOG + Dex nanoparticles performed significantly better than PBS, empty nanoparticles, Dex nanoparticles, MOG nanoparticles, or free Dex + MOG.[31] Mechanistically, we show that mice treated with hPG_{K4}-Dex liposomes had a significantly lower proportion of $\%CD11c^+CD86^+$ DCs compared to the PBS group (Figure 4A). At the same time, there was a greater amount of $CD4^+CD25^+Foxp3^+$ and $CD4^+PD\text{-}1^+$ T cells in the spleens of these mice (Figure 4C and D). This suggests that there were some long-lasting systemic effects of the therapy. However, it is unknown whether these cells contributed to protection against arthritis or are the result of reduced inflammation in mice. The effect does seem to be antigen-specific since it was not observed in the mice receiving OVA_{323K4}-Dex liposomes. Further studies should be performed to unravel this. Nguyen et al. also observed a decrease in $CD86^+$ APCs and an increase in $Foxp3^+CD4^+$ T cells in the spleens of mice after nanoparticle treatment, which coincided with protection against EAE.[56] Interestingly, we saw a significant increase in the expression of *IL10* in the paws of mice treated with hPG_{K4}-Dex liposomes (Figure 4J), which likely explains why these mice had a lower arthritis score than controls.[57,58]

Liposomes have been used as delivery vehicles to target Dex toward the inflamed joints, thereby reducing arthritis symptoms through the broad inflammation-inhibiting properties of Dex. To test the antigen-specificity of our treatment, and the effect of delivering liposomal Dex in arthritis mice, we treated mice with OVA_{323K4}-Dex liposomes, OVA_{323} being a disease-irrelevant MHC-II antigen. We observed no changes in any assays between OVA_{323K4}-Dex liposomes compared to PBS (Figures 3 and 4). This was expected, since to obtain an accumulation of liposomes in inflamed joints through the leaky vasculature that is associated with inflammation,[59] it is necessary to functionalize the liposomes through, for example, PEGylation,[60] peptides,[61] or other small molecules[62] on the surface of the liposomes. Furthermore, the dose of Dex reported in studies that deliver Dex to the site of inflammation via nanoparticles is 5 to 30 times higher than the dose used in this study (0.1–1.2 mg kg^{-1} versus 0.02 mg kg^{-1}), and often requires more than 2 injections. Therefore, we can conclude that the observed effect in our study is not due to the accumulation of Dex liposomes in the joints that affect the inflamed tissue, but rather due to antigen-specific skewing of T cells toward protective responses against arthritis.

Since the hPG_{K4}-Dex conjugates are amphipathic molecules, they could potentially self-assemble into micelles or nanoparticles during the fabrication process of the liposomes. During the formulation and characterization process, we did not observe such particles forming, most likely due to the low concentration of hPG_{K4}-Dex conjugates used, although we do not know what the critical micellar concentration of the conjugates is. Further studies are required to assure that the purification through ultracentrifugation would eliminate the self-assembled particles and their potential in vivo effects.

More research is required for translation to human studies. However, the liposomes are similar to a formulation that is already approved in humans[63] and dexamethasone is a commonly prescribed drug.[64] Furthermore, we propose that the liposomes result in a large dose-reduction of dexamethasone, which would suggest that the therapy is safe to use in humans. The antigen chosen in this study was hPG since it is used to induce arthritis in the mouse model, however, in human patients, we would likely require a different antigen, such as (citrullinated) peptides derived from fibrinogen, vimentin and collagen, or heat shock protein (HSP)70.[65] The only clinical trial carried out so far with a similar treatment strategy for rheumatoid arthritis showed that the liposomes were well-tolerated and induced T cells with tolerogenic TCR signaling and exhaustion profiles.[66]

The liposomes in combination with our novel antigen-Dex conjugates provide a promising strategy to inhibit arthritis development. The results presented here highlight the therapeutic potential of antigen-Dex-loaded DSPG-containing liposomes in immune therapy against autoimmune diseases.

4. Experimental Section

Synthesis and Characterization of Dex-peptide Conjugates: Preloaded Fmoc-Lys(Boc)-Wang resin, Fmoc-Arg(Pbf)-Wang resin, 9-fluorenylmethyloxycarbonyl (Fmoc)-protected amino acids, and trifluoroacetic acid (TFA) were purchased from Novabiochem GmbH (Hohenbrunn, Germany). Peptide grade dimethylformamide (DMF), dichloromethane (DCM), piperidine, *N, N'*-diisopropyl carbodiimide (DIC), and high-performance liquid chromatography (HPLC) grade acetonitrile were purchased from Biosolve BV (Valkenswaard, Nether-

lands). Ethyl cyanohydroxyiminoacetate (Oxyma pure) was purchased from Manchester Organics Ltd (Cheshire, UK). Triisopropylsilane (TIPS), BioUltra grade ammonium bicarbonate, succinyl anhydride, 4-dimethylaminopyridine (DMAP), and pyridine were purchased from Sigma-Aldrich Chemie BV (Zwijndrecht, Netherlands). Dex was purchased from Acros Organics BV (Hague, Netherlands).

Dex-peptide conjugates were synthesized as described previously.[38] In brief, the peptide epitope sequences were synthesized by microwave-assisted Fmoc-based chemistry using an H12 liberty blue peptide synthesizer (CEM Corporation, US). Dex succinate was coupled to the N-terminal of the peptide as with other Fmoc-protected amino acids. TFA/water/TIPS (95/2.5/2.5) was used to cleave the peptide off the resin and remove the side chain protecting groups. Peptides were purified by Prep-HPLC using Reprosil-Pur C18 column (10 µm, 250 × 22 mm). Mass spectrometry (MS) analysis was performed using a Bruker microTOF-Q instrument in positive mode to confirm the identity of the synthetic products. The epitope was derived from the hPG and Ovalbumin (OVA) antigens with the sequence ATEGRVRVNSAYQDK and ISQAVHAAHAEINEAGR, respectively. A lysine tetramer was added to the N-terminal of the epitope sequences for the introduction of a cationic charge. A biodegradable succinyl spacer was added to Dex before conjugation to the N-terminus of the peptide on resin. The Dex-peptide conjugates were cleaved and purified as described above for the peptides.

Liposome Preparation and Characterization: Liposomes were prepared using the thin film hydration followed by extrusion method. The phospholipids 1,2-distearoyl-sn-glycero-3-phosphocholine (DSPC) and 1,2-distearoyl-sn-glycero-3-phosphoglycerol (DSPG), were purchased from Avanti Polar Lipids, Birmingham, AL, USA. Cholesterol (CHOL) was purchased from Sigma-Aldrich. Briefly, 180 mg total of dry powder DSPC:DSPG:CHOL in a 4:1:2 molar ratio was weighed and transferred to a dry 100 mL round-bottom flask. The lipids were dissolved in 8 mL chloroform and 8 mL methanol. The solvents were evaporated under a vacuum in a rotary evaporator for 1 h at 40 °C, followed by an N_2 stream for 30 min at RT. The resulting lipid film was rehydrated with 2000 µg of hPG, hPG_{K4}, hPG_{K4}-Dex or OVA_{323K4}-Dex dissolved in 10 mM 4-(2-hydroxyethyl)−1-piperazineethanesulfonic acid (HEPES, pH 7.2) buffer to a total volume of 4 mL and homogenized by rotation in a water bath at 40 °C for 1 h. For empty liposomes, liposomes were rehydrated with 4 mL of 10 mM HEPES buffer. The resulting suspension was sized by high-pressure extrusion (LIPEX Extruder, Northern Lipids Inc., Burnaby, BC, Canada) on a heating plate set at 60 °C by passing the dispersion four times through stacked 400 and 200 nm pore-size membranes (Whatman NucleoporeTM, GE Healthcare, Amersham, UK). To separate non-encapsulated cargo from the liposomes, liposomes were ultracentrifuged (Type 70.1 Ti rotor) for 35 min at 55 000 rpm at 4 °C. Liposomes were washed with 10 mL HEPES buffer and centrifugation was repeated three times. Liposomes were stored at 4 °C and their stability was measured periodically. Liposomes were used within 2 months for in vitro experiments and within 2 weeks for in vivo experiments.

The Z-average diameter and polydispersity index (PDI) of the liposomes were measured by dynamic light scattering (DLS) using a NanoZS Zetasizer (Malvern Ltd., Malvern, UK). For this, 10 µL of liposomes were diluted in 990 µL HEPES buffer pH 7.2. The ζ-potential was measured by laser Doppler electrophoresis (Malvern Ltd.) using a universal dip cell. To determine the concentration of loaded hPG_{K4}, hPG_{K4}-Dex, $OVA_{323K4,}$ or OVA_{323K4}-Dex RP-UPLC was used. For this, 20 µL of liposome suspension was dissolved in 180 µL of methanol, and the sample was vortexed. Sample injections were 7.5 µL in volume and the column used was a 1.7 µm BEH C18 column (2.1 × 50 mm, Waters ACQUITY UPLC, Waters, MA, USA). Column and sample temperatures were 40 and 20 °C, respectively. The mobile phases were Milli-Q water with 0.1% TFA (solvent A) and acetonitrile with 0.1% TFA (solvent B). For separation, the mobile phases were applied in a linear gradient from 5% to 95% solvent B over 10 min at a flow rate of 0.25 mL min^{-1}. Peptide content was detected by absorbance at 280 nm, and Dex was detected at 240 nm[39] using an ACQUITY UPLC TUV detector (Waters ACQUITY UPLC, Waters, MA, USA). Peptide concentrations were calculated based on the respective calibration curves of antigen-Dex complexes dissolved in Milli-Q water.

Mice: For bone marrow isolation, 8-week-old WT mice on Balb/cAnNCrl background (male and female) were purchased from Charles River laboratories. $Tyh1.1^+$ hPG-TCR transgenic[40] mice were bred in-house at the central animal laboratory of Utrecht University, the Netherlands. For proteoglycan-induced arthritis (PGIA) studies, 16-week-old female Balb/cAnNCrl mice were purchased from Charles River laboratories. Mice were randomized into experimental groups based on weight or arthritis score using RandoMice.[41] Humane end-points were adhered to, and the physical discomfort of arthritic animals was relieved by providing easy-to-reach water and food, and additional soft bedding materials. Animals were kept under standard conditions of the animal facility and all experiments were approved by the Animal Experiment Committee of Utrecht University (AVD108002016467 and AVD10800202115687).

Murine Bone Marrow-Derived Dendritic Cell Isolation, Dendritic Cell Culture, and Stimulation: Bone marrow isolated from femurs and tibias of Balb/cAnNCrl WT mice were homogenized and seeded in 6-well plates at a cell density of 450 000 cells mL^{-1} in 2 mL IMDM (Gibco, ThermoFisher Scientific) supplemented with 10% FCS (Fetal Calf Serum; Bodinco, Alkmaar, The Netherlands), 100 units mL^{-1} of penicillin (Gibco, ThermoFisher Scientific, Landsmeer, The Netherlands), 100 ug mL^{-1} of streptomycin (Gibco, ThermoFisher Scientific, Landsmeer, The Netherlands) and 0.5 µM β-mercaptoethanol (Gibco, ThermoFisher Scientific, Landsmeer, The Netherlands). Cells were cultured at 37 °C and 5% CO_2 in the presence of 20 ng mL^{-1} of granulocyte-macrophage colony-stimulating factor (GM-CSF, in-house produced) for 6 days. On day 2, IMDM and 20 ng mL^{-1} GM-CSF were added to the wells. Extra GM-CSF (20 ng mL^{-1}) was supplemented on day 5. On day 6, cells were harvested by scraping and counted. For flow cytometry of DCs, and further co-culture with T cells, cells were transferred to a 96-well F-bottom plate at 50 000 cells $well^{-1}$. The cells were left to adhere for 2 h. Cells were matured in the presence of 10 ng mL^{-1} lipopolysaccharide (LPS, O111:B4; Sigma-Aldrich) and treated with free or encapsulated hPG_{K4}, or free or encapsulated hPG_{K4}-Dex (200 µL $well^{-1}$). In all cases, the concentration of the peptide was 1 ug mL^{-1}. For Dex-containing groups, the concentration was 0.18 ug mL^{-1} Dex. After 16 h, DCs were harvested for phenotypic characterization by flow cytometry. For qPCR and ELISA, cells were plated out at 600 000 cells $well^{-1}$ in an F-bottom 48-well plate. The cells were left to adhere for 2 h. Cells were stimulated with the same conditions and concentrations as for flow cytometry, in a total volume of 600 µL $well^{-1}$.

Human Monocyte Isolation, Monocyte-Derived Dendritic Cell Culture, and Stimulation: Peripheral blood mononuclear cells (PBMCs) were obtained from healthy human donors at Sanquin Blood Bank (Amsterdam, Netherlands). Informed consent was given in accordance with the Declaration of Helsinki and Dutch National and Sanquin Internal Ethic Boards. PBMCs were isolated by a Ficoll gradient, and subsequently, monocytes were isolated using anti-CD14 microbeads (Miltenyi Biotech) according to the manufacturer's instructions. Monocytes were seeded in 6-well plates at 2 000 000 cells mL^{-1} in 2 mL RPMI (Gibco) supplemented with 5% FCS (Bodinco, Alkmaar, The Netherlands), 100 units mL^{-1} of penicillin (Gibco, ThermoFisher Scientific, Landsmeer, The Netherlands), and 100 ug mL^{-1} of streptomycin (Gibco, ThermoFisher Scientific, Landsmeer, The Netherlands). To differentiate monocytes toward DCs, 50 ng mL^{-1} hGM-CSF (Miltenyi Biotech) and 50 ng mL^{-1} hIL-4 (Miltenyi Biotech) were added. On day 3 of culture, fresh medium, and cytokines were added. On day 6, cells were harvested by scraping, counted, and transferred to a 96-well F-bottom plate at 50 000 cells $well^{-1}$. The cells were left to adhere for 2 h. Cells were matured in the presence of 100 ng mL^{-1} lipopolysaccharide (LPS, O111:B4; Sigma-Aldrich) and treated with free or encapsulated hPG_{K4}, or free or encapsulated hPG_{K4}-Dex (200 µL $well^{-1}$). In all cases, the concentration of the peptide was 1 ug mL^{-1}. For Dex-containing groups, the concentration was 0.18 ug mL^{-1} Dex. After 16 h, DCs were harvested for phenotypic characterization by flow cytometry.

Enrichment of CD4+ T cells from Murine Spleens and Co-Culture with BMDCs: Spleens were isolated from $Thy1.1^+$ hPG-TCR mice. A single-cell suspension of splenocytes was obtained by mashing spleens through a 70 µM filter (Falcon, Corning, New York, USA). Erythrocytes were lysed with Ammonium–Chloride–Potassium (ACK) lysis buffer (0.15 M NH4Cl,

1 mM KHCO3, 0.1 mM Na2EDTA; pH 7.3). $CD4^+$ T cells were negatively selected by magnetic separation using Dynabeads (sheep anti-rat IgG, ThermoFisher) and anti-CD8 (YTS169), anti-CD11b (M1/70), anti-MHCII (M5/114) and anti-B220 (RA3-6B2, all in-house produced). The enriched $CD4^+$ T cells were labeled with carboxyfluorescein succinimidyl ester (CFSE, 0.5 nM) according to the manufacturer's protocol (ThermoFisher). BMDCs were plated out into a 96-well F-bottom plate (50 000 cells $well^{-1}$) and stimulated as described above. After 16 h stimulation, cells were washed four times with 200 µL PBS/well to remove any free stimuli. To this, 100 000 cells $well^{-1}$ of CFSE-labelled $CD4^+$ T cells suspended in 200 µL RPMI (Gibco), supplemented with 5% FCS (Bodinco, Alkmaar, The Netherlands), 100 units mL^{-1} of penicillin (Gibco, ThermoFisher Scientific, Landsmeer, The Netherlands), and 100 ug mL^{-1} of streptomycin (Gibco, ThermoFisher Scientific, Landsmeer, The Netherlands) were added and incubated for 3 days. Subsequently, $CD4^+$ T cells were harvested for phenotypic characterization by flow cytometry.

Inflammatory Adoptive Transfer In Vivo: $CD4^+$ T cells were purified from the spleens and lymph nodes of $Thy1.1^+$ hPG-TCR transgenic mice as described above. At t0, WT Balb/cAnNCrl mice received an intramuscular injection of 50 uL PBS containing 100ug hPG protein to induce a strong inflammatory response against hPG. After 2 h mice received 50 0000 $CD4^+$ T cells intravenous via the tail vein. After 16 h, mice were immunized intravenously with 200 uL PBS, 1 nmol free hPG_{K4}, 1 nmol hPG_{K4} liposomes, or 1 nmol hPG_{K4}-Dex liposomes. 3 days after immunization, mice were sacrificed, and spleens were removed and processed as described above.

Preventative Arthritis Study In Vivo: To induce arthritis in mice, female Balb/cAnNCrl mice were injected on days 0 and 21 intraperitoneally with a mixture of 2 mg dimethyldiotadecylammonium bromide (DDA) and 250 µg human proteoglycan. For the treatment of mice with hPG_{K4}-Dex tolDCs, BMDCs were cultured in 6-well plates as described above. On day 6, 40 ug mL^{-1} hPG_{K4}-Dex and 10 ng mL^{-1} LPS were added to the cells. DCs were harvested after 16 h. The viability, purity, and phenotype of the DCs were confirmed using flow cytometry before injection in mice. Mice were treated on day 17 via an intravenous injection in the tail vein with 200 µL PBS, 200 µL 1×10^6 hPG_{K4}-Dex tolDCs (equivalent to 20 nmol of hPG_{K4}-Dex) in PBS, or 200 µL hPG_{K4}-Dex liposomes (2 nmol hPG_{K4}-Dex) in PBS. Arthritis scores were determined three times per week starting from day 21 until day 55 in a blinded fashion by two researchers independently using a visual scoring system based on swelling and redness of paws.[42] At the end of the experiment, mice were sacrificed by cervical dislocation.

Curative Arthritis Study In Vivo: To induce arthritis in mice, female Balb/cAnNCrl mice were injected twice intraperitoneally with a mixture of 2 mg DDA and 250 µg human proteoglycan as described above. Arthritis scores were determined three times per week as described above. Mice were enrolled in the experiment (day −1) when they had a score of >2 for 2 consecutive scoring moments. Mice were treated on days 0 and 7 via intravenous injection in the tail vein with 200 µL PBS, 200 µL hPG_{K4}-Dex liposomes (2 nmol hPG_{K4}-Dex) in PBS, or 200 µL OVA_{K4}-Dex liposomes (2 nmol OVA_{323K4}-Dex) in PBS. Mice were scored during a period of 25 days after enrollment. At the end of the experiment, mice were sacrificed by cervical dislocation. Spleens were collected for flow cytometry, paws were collected for qPCR, and blood was collected for ELISA in 0.8 mL z-serum separation tubes (Greiner Bio-One, Kremsmünster, Austria). Serum was separated from cells by centrifuging the blood samples at 10 000× g for 5 min at 4 °C, collected into separate tubes, and stored at −20 °C.

ELISA of Stimulated BMDCs: BMDCs were stimulated as described above and the supernatant was harvested and either used directly for ELISA or stored at −80 °C for future analysis. IL-10 (U-CyTech, Utrecht, the Netherlands) and IL-12p70 (9A5 and C17.8, BD Biosciences) was measured in the supernatants by ELISA according to the manufacturer's instructions. Briefly, F-bottom Costar assay 96-well plates (Corning, Kennebunk, ME, USA) were coated with capture antibody at 4 °C overnight. Plates were washed thoroughly with 0.01% Tween-20 in PBS and blocked with 1% BSA in PBS for 30 min at RT. Subsequently, plates were washed, and (diluted) samples and standard curves were incubated for 2 h at RT. Then, plates were washed and the biotinylated detection antibody and streptavidin-HRP (BD Biosciences) were incubated for 1 h at RT. Finally, plates were washed, and the samples were reacted with TMB substrate solution (BioLegend). The reaction was stopped with 2 N H_2SO_4 solution, and the plates were measured using an iMark Microplate Absorbance Reader (Bio-Rad). Cytokine concentrations were calculated based on the respective calibration curves prepared with purified cytokines.

qPCR of Stimulated BMDCs: BMDCs were stimulated as described above, and 350 µL RLT buffer (Qiagen Benelux B.V., Venlo, the Netherlands) was added to the cells. The lysate was either used directly for mRNA extraction or stored at −80 °C for future analysis. Total mRNA was extracted from stimulated BMDCs using the RNeasy kit (Qiagen) according to the manufacturer's instructions. DNase treatment was performed on-column (Qiagen). The yield of mRNA extraction was measured using a Nanodrop (ThermoFisher). Transcription into cDNA was performed using the iScript cDNA Synthesis Kit (Bio-Rad Laboratories B.V., Veenendaal, The Netherlands). PCR and Real-Time detection were performed using a Bio-Rad MyiQ iCycler (Bio-Rad). Amplification was performed using IQ SYBR Green Supermix (Bio-Rad) with 0.25 µM final concentrations of primers specific for *IL1B* (5′-TCC ATC TTC TTC TTT GGG TAT TG-3′ and 5′-TTC CCG TGG ACC TTC CAG-3′) and Indoleamine 2,3-dioxygenase 1 *(IDO)* (5′-GCA GAC TGT GTC CTG GCA AAC T-3′ and 5′-AGA GAC GAG GAA GAA GCC CTT G-3′), and hypoxanthine-guanine phosphoribosyl transferase (*HPRT*) (5′-CTG GTG AAA AGG ACC TCT CG-3′ and 5′-TGA AGT ACT CAT TAT AGT CAA GGG CA-3′). The following PCR program was used: pre-soaking at 95 °C for 3 min, [denaturation at 95 °C for 20 s, annealing at 59 °C for 30 s] repeated 40 times. Melting curves and primer efficiencies were measured for each sample. For each sample mRNA expression was normalized to the detected C_t value of *HPRT* and expressed relative to the average of the DCs incubated with hPG_{K4} + LPS.

qPCR of Paws: Paws were harvested and pooled per mouse in 6-well plates containing ice-cold sterile PBS. The skin was removed using scissors and tweezers, and the paws were agitated to release synovial fluid. The resulting suspension was passed through a 70 µM filter (Falcon, Corning, New York, USA) and cells were pelleted by centrifugation. After the removal of supernatant, cells were lysed using 350 µL RLT buffer (Qiagen Benelux B.V., Venlo, the Netherlands). Total mRNA was immediately extracted using the RNeasy kit (Qiagen) according to the manufacturer's instructions. Transcription into cDNA was performed using the iScript cDNA Synthesis Kit (Bio-Rad Laboratories B.V., Veenendaal, The Netherlands). PCR and Real-Time detection were performed using a Bio-Rad MyiQ iCycler (Bio-Rad). Amplification was performed using IQ SYBR Green Supermix (Bio-Rad) with 0.25 µM final concentrations of primers specific for *MPO* (5′-GCT ACC CGC TTC TCC TTC TT-3′ and 5′-GGT TCT TGA TTC GAG GGT CA-3′), *IL1B* (5′- TCC ATC TTC TTC TTT GGG TAT TG-3′ and 5′-TTC CCG TGG ACC TTC CAG-3′), *IL10* (5′-GGT TGC CAA GCC TTA TCG GA-3′ and 5′-ACC TGC TCC ACT GCC TTG CT-3′), and hypoxanthine-guanine phosphoribosyl transferase (*HPRT*) (5′-CTG GTG AAA AGG ACC TCT CG-3′ and 5′-TGA AGT ACT CAT TAT AGT CAA GGG CA-3′). The following PCR program was used: pre-soaking at 95 °C for 3 min, [denaturation at 95 °C for 20 s, annealing at 59 °C for 30 s] repeated 40 times. Melting curves and primer efficiencies were measured for each sample. The Pfaffl method was used to calculate the gene expression ratio of each gene of interest versus HPRT, using the PBS group as control.

ELISA of Serum Anti-hPG IgG1 and IgG2a: ELISA 96-well plates (Corning) were coated overnight with hPG (5 µg mL^{-1} per well) in 0.1 M Carbonate buffer (pH = 9.5). Subsequently, wells were blocked with a blocking buffer consisting of 1.5% milk powder (Campina, Zaltbommel, The Netherlands) dissolved in 1X PBS for 2 h at RT. Mouse serum was added to the wells at different dilutions (IgG1: 1:12 500, 1:25 000, 1:50 000; IgG2a: 1:500, 1:2500, 1:12 500). On each plate, a standard curve composed of serum of a mouse that reached the humane endpoint for arthritis development (PGIA induction, no treatment) at dilutions 0, 1:6250, 1:12 500, 1:25 000, 1:50 000, 1:100 000 for IgG1 and 0, 1:250, 1:500, 1:1000, 1:2000, 1:4000 for IgG2a was included. After 2 h, IgG1-HRP (X56; BD Biosciences) and IgG2a-HRP(19-15; BD Biosciences) antibodies were added to the wells in the blocking buffer at a 1:1000 dilution. After 1 h of incubation at RT, wells were washed, and TMB (Thermo Fisher Scien-

tific) was added. The reaction was stopped using 2 M H_2SO_4. ELISA data was read on the using an iMark Microplate Absorbance Reader (Bio-Rad) at 450 nm. The background signal (550 nm) was subtracted and serum levels of anti-hPG IgG1 and IgG2a were calculated using the standard curve.

Flow Cytometry: BMDCs or moDCs were stimulated as described above and harvested, washed three times with 200 µL of 4 mM EDTA and once with 200 µL PBS to remove any free antigen or liposomes, and transferred to a V-bottom 96-well plate. Co-cultured CFSE-labelled $CD4^+$ T cells were harvested and transferred to a V-bottom 96-well plate. For splenocytes from in vivo experiments, 2×10^6 splenocytes were plated out in 96-well U-bottom plates.

Cell suspensions were blocked for 15 min with 10 ug mL^{-1} Fc Block (2.4G2, in-house produced). BMDCs were stained with a monoclonal antibody mix of CD11c-APC (N418, eBioscience, Thermo Fisher Scientific), TLR2-FITC (6C2, eBioscience, Thermo Fisher Scientific), CD86-FITC (GL1, BD Biosciences), CD40-PE (3/23, BD Biosciences), LAP-PE (TW7-16B4, eBioscience, Thermo Fisher Scientific), MerTK-APC (2B10C42, BioLegend), and ViaKrome808 (Beckman Coulter, Indianapolis, IN, USA) in FACS Buffer (1X PBS supplemented with 2% FCS, 0.01% sodium azide, and 2 mM EDTA). moDCs were stained with a monoclonal antibody mix of CD11c-PE (MJ4-27G12, Miltenyi), CD40 PE-Cy7 (5C3, eBioscience), CD86-BB515 (FUN-1, BD Biosciences), and ViaKrome808 (Beckman Coulter, Indianapolis, IN, USA) in FACS Buffer. $CD4^+$ T cells were stained with a monoclonal antibody mix of CD4-BV785 (RM4-5, BioLegend, USA), LAG-3-PE (eBioC9B7W, eBioscience, Thermo Fisher Scientific, USA), CD49b-APC-Cy7 (DX5, BioLegend, USA), and CD25-PerCP-Cy5.5 (PC61.5, eBioscience, Thermo Fisher Scientific, USA), and ViaKrome808 (Beckman Coulter, Indianapolis, IN, USA) in FACS Buffer. After 30 min incubation at 4 °C in the dark, cells were washed with PBS, and fixed and permeabilized using the FoxP3 transcription factor staining set (eBioscience, San Diego, CA, USA). Subsequently, cells were stained intracellularly according to the manufacturer's instructions with FoxP3-eFluor450 (FJK-16s, eBioscience, Thermo Fisher Scientific) and T-Bet-APC (4B10, eBioscience, Thermo Fisher Scientific). Splenocytes from the adoptive transfer experiment were stained with CD4-BV510 (RM4-5, BioLegend, USA), Thy1.1-PerCP-Cy5.5 (HIS51, eBioscience), Thy1.1-FITC (HIS51, eBioscience), LAG-3-APC (C9B7W, eBioscience), CD49b-APC-Cy7 (DX5, Biolegend), PD-L1-BV650 (10F.9G2, Biolegend), CD11c-FITC (N418, eBioscience), CD86-PE-Cy5 (GL1, eBioscience), and ViaKrome808 (Beckman Coulter, Indianapolis, IN, USA) in FACS Buffer. After 30 min incubation at 4 °C in the dark, cells were washed with PBS, and fixed and permeabilized using the FoxP3 transcription factor staining set (eBioscience, San Diego, CA, USA). Subsequently, cells were stained intracellularly according to the manufacturer's instructions with FoxP3-eFluor450 (FJK-16s, eBioscience, Thermo Fisher Scientific) and T-bet-APC (4B10, eBioscience). Splenocytes from the curative arthritis study experiment were stained with a monoclonal antibody mix of CD4-BV785 (RM4-5, BioLegend, USA) and CD25-PerCPCy5.5 (PC61.5, eBioscience, Thermo Fisher Scientific, USA), and ViaKrome808 (Beckman Coulter, Indianapolis, IN, USA) in FACS Buffer. After 30 min incubation at 4 °C in the dark, cells were washed with PBS, and fixed and permeabilized using the FoxP3 transcription factor staining set (eBioscience, San Diego, CA, USA). Subsequently, cells were stained intracellularly according to the manufacturer's instructions with FoxP-eFluor450 (FJK-16s, eBioscience, Thermo Fisher Scientific), RORγT-PE (AFKJS-9, eBioscience, Thermo Fisher Scientific), GATA-3-PE-Cy7 (TWAJ, eBioscience, Thermo Fisher Scientific) and T-Bet-APC (4B10, eBioscience, Thermo Fisher Scientific). After 30 min incubation at 4 °C in the dark, cells were washed and resuspended in 100 µL PBS for measurement. To ensure correct analysis, relevant single-stain, and fluorescence minus one (FMO) controls were used. Samples were measured on a Beckman Coulter Cytoflex LX at the Flow Cytometry and Cell Sorting Facility located at the Faculty of Veterinary Medicine at Utrecht University. The total measured volume was 85 µL per sample, at a measurement speed of 60 µL min^{-1}. Acquired data were analyzed using FlowJo Software v.10.7 (FlowJo LLC, Ashland, OR, USA).

Statistical analysis: Statistical analysis was performed in GraphPad Prism v.9.3.1. Details of the analyses are indicated in the figure legends.

Supporting Information

Supporting Information is available from the Wiley Online Library or from the author.

Acknowledgements

N.B. and D.ter B. contributed equally to this work. The authors would like to thank Dr. I. S. Ludwig and Dr. A. J. Stoppelenburg for helpful discussions and help during the animal studies. Graphics in the graphical abstract and Figure 3 were created in Biorender.com. This work was funded in part by the DC4Balance collaboration project. which is co-funded by the PPP Allowance made available by Health~Holland, Top Sector Life Sciences and Health, to the Dutch Cooperation of Health Foundations (SGF) and the Dutch Arthritis Foundation. Declaration of Generative AI and AI-assisted technologies in the writing process: The authors did not use generative AI or AI-assisted technologies during any stage in the writing process.

Conflict of Interest

The authors declare no conflict of interest.

Data Availability Statement

The data that support the findings of this study are available from the corresponding author upon reasonable request.

Keywords

autoimmunity, dexamethasone, immunotherapy, liposomes, rheumatoid arthritis

Received: November 30, 2023
Revised: January 23, 2024
Published online: February 11, 2024

[1] K. Almutairi, J. Nossent, D. Preen, H. Keen, C. Inderjeeth, *Rheumatol. Int.* **2021**, *41*, 863.
[2] J. S. Smolen, D. Aletaha, A. Barton, G. R. Burmester, P. Emery, G. S. Firestein, A. Kavanaugh, I. B. McInnes, D. H. Solomon, V. Strand, K. Yamamoto, *Nat. Rev. Dis. Primers* **2018**, *4*, 18001.
[3] J. Y. Han, M. A. Reynolds, *J. Periodontal Implant Sci.* **2012**, *42*, 3.
[4] S. Shams, J. M. Martinez, J. R. D. Dawson, J. Flores, M. Gabriel, G. Garcia, A. Guevara, K. Murray, N. Pacifici, M. V. Vargas, T. Voelker, J. W. Hell, J. F. Ashouri, *Front. Pharmacol.* **2021**, *12*, 680043.
[5] M. Her, A. Kavanaugh, *J. Allergy Clin. Immunol.* **2016**, *137*, 19.
[6] L. Passeri, F. Marta, V. Bassi, S. Gregori, *Int. J. Mol. Sci.* **2021**, *22*, 8415.
[7] C. M. U. Hilkens, J. D. Isaacs, *Clin. Exp. Immunol.* **2013**, *172*, 148.
[8] A. Page, F. Fusil, F. L. Cosset, *Joint Bone Spine* **2021**, *88*, 105164.
[9] M. P. Domogalla, P. V. Rostan, V. K. Raker, K. Steinbrink, *Front. Immunol.* **2017**, *8*, 01764.
[10] K. Steinbrink, E. Graulich, S. Kubsch, J. Knop, A. H. Enk, *Blood* **2002**, *99*, 2468.
[11] M. A. A. Jansen, R. Spiering, I. S. Ludwig, W. van Eden, C. M. U. Hilkens, F. Broere, *Front. Immunol.* **2019**, *10*, 02068.
[12] K. Kretschmer, I. Apostolou, D. Hawiger, K. Khazaie, M. C. Nussenzweig, H. von Boehmer, *Nat. Immunol.* **2005**, *6*, 1219.
[13] I. Apostolou, H. Von Boehmer, *J. Exp. Med.* **2004**, *199*, 1401.

[14] N. L. Harris, F. Ronchese, *Immunol. Cell Biol.* **1999**, *77*, 304.
[15] I. Vogel, B. Verbinnen, W. Maes, L. Boon, S. W. Van Gool, J. L. Ceuppens, *Eur. J. Immunol.* **2013**, *43*, 1013.
[16] P. A. García-González, K. Schinnerling, A. Sepúlveda-Gutiérrez, J. Maggi, A. M. Mehdi, H. J. Nel, B. Pesce, M. L. Larrondo, O. Aravena, M. C. Molina, D. Catalán, R. Thomas, R. A. Verdugo, J. C. Aguillón, *Front. Immunol.* **2017**, *8*, 01350.
[17] J. Navarro-Barriuso, M. J. Mansilla, M. Naranjo-Gómez, A. Sánchez-Pla, B. Quirant-Sánchez, A. Teniente-Serra, C. Ramo-Tello, E. M. Martínez-Cáceres, *Sci. Rep.* **2018**, *8*, 14985.
[18] D. T. Braake, N. Benne, C. Y. J. Lau, E. Mastrobattista, F. Broere, *Pharmaceutics* **2021**, *13*, 1949.
[19] B. Willekens, S. Presas-Rodríguez, M. J. Mansilla, J. Derdelinckx, W.-P. Lee, G. Nijs, M. De Laere, I. Wens, P. Cras, P. Parizel, W. Van Hecke, A. Ribbens, T. Billiet, G. Adams, M.-M. Couttenye, J. Navarro-Barriuso, A. Teniente-Serra, B. Quirant-Sánchez, A. Lopez-Diaz de Cerio, S. Inogés, F. Prosper, A. Kip, H. Verheij, C. C. Gross, H. Wiendl, M. S. Van Ham, A. T. Brinke, A. M. Barriocanal, A. Massuet-Vilamajó, N. Hens, et al., *BMJ Open* **2019**, *9*, 030309.
[20] G. M. Bell, A. E. Anderson, J. Diboll, R. Reece, O. Eltherington, R. A. Harry, T. Fouweather, C. MacDonald, T. Chadwick, E. McColl, J. Dunn, A. M. Dickinson, C. M. U. Hilkens, J. D. Isaacs, *Ann. Rheum. Dis.* **2017**, *76*, 227.
[21] B. E. Phillips, Y. Garciafigueroa, C. Engman, M. Trucco, N. Giannoukakis, *Front. Immunol.* **2019**, *10*, 00148.
[22] B. E. Phillips, Y. Garciafigueroa, M. Trucco, N. Giannoukakis, *Front. Immunol.* **2017**, *8*, 01279.
[23] N. Benne, D. ter Braake, A. J. Stoppelenburg, F. Broere, *Front. Immunol.* **2022**, *13*, 864403.
[24] T. K. Kishimoto, R. A. Maldonado, *Front. Immunol.* **2018**, *9*, 00230.
[25] C. Krienke, L. Kolb, E. Diken, M. Streuber, S. Kirchoff, T. Bukur, O. Akilli-Ozturk, L. M. Kranz, H. Berger, J. Petschenka, M. Diken, S. Kreiter, N. Yogev, A. Waisman, K. Kariko, O. Tureci, U. Sahin, *Science* **2021**, *371*, 145.
[26] S. T. Schmidt, C. Foged, K. S. Korsholm, T. Rades, D. Christensen, *Pharmaceutics* **2016**, *8*, 7.
[27] B. S. Pattni, V. V. Chupin, V. P. Torchilin, *Chem. Rev.* **2015**, *115*, 10938.
[28] D. Guimarães, A. Cavaco-Paulo, E. Nogueira, *Int. J. Pharm.* **2021**, *601*, 120571.
[29] N. Benne, J. van Duijn, F. Lozano Vigario, R. J. T. Leboux, P. van Veelen, J. Kuiper, W. Jiskoot, B. Slütter, *J. Controlled Release* **2018**, *291*, 135.
[30] S.-H. Kim, J.-H. Moon, S. U. Jeong, H.-H. Jung, C. S. Park, B. Y. Hwang, C.-K. Lee, *Int. J. Nanomed.* **2019**, *14*, 5229.
[31] K. J. Peine, M. Guerau-de-Arellano, P. Lee, N. Kanthamneni, M. Severin, G. D. Probst, H. Peng, Y. Yang, Z. Vangundy, T. L. Papenfuss, A. E. Lovett-Racke, E. M. Bachelder, K. M. Ainslie, *Mol. Pharmaceutics* **2014**, *11*, 828.
[32] C. Q. Xia, R. Peng, F. Beato, M. J. Clare-Salzler, *Scand. J. Immunol.* **2005**, *62*, 45.
[33] J. Visser, A. van Boxel-Dezaire, D. Methorst, T. Brunt, E. R. de Kloet, L. Nagelkerken, *Blood* **1998**, *91*, 4255.
[34] T. Rhen, J. A. Cidlowski, *N. Engl. J. Med.* **2005**, *353*, 1711.
[35] V. A. Tsotas, S. Mourtas, S. G. Antimisiaris, *Drug Deliv.* **2007**, *14*, 441.
[36] U. Bhardwaj, D. J. Burgess, *Int. J. Pharm.* **2010**, *388*, 181.
[37] V. S. Madamsetty, R. Mohammadinejad, I. Uzieliene, N. Nabavi, A. Dehshahri, J. García-Couce, S. Tavakol, S. Moghassemi, A. Dadashzadeh, P. Makvandi, A. Pardakhty, A. Aghaei Afshar, A. Seyfoddin, *ACS Biomater. Sci. Eng.* **2022**, 1763.
[38] C. Y. J. Lau, N. Benne, B. Lou, O. Zharkova, H. J. Ting, D. ter Braake, N. van Kronenburg, M. H. Fens, F. Broere, W. E. Hennink, J.-W. Wang, E. Mastrobattista, *J. Controlled Release* **2022**, *348*, 938.
[39] L. Xue, D. Wang, X. Zhang, S. Xu, N. Zhang, *Int. J. Pharm.* **2020**, *586*, 119642.
[40] S. E. Berlo, P. J. van Kooten, C. B. ten Brink, F. Hauet-Broere, M. A. Oosterwegel, T. T. Glant, W. Van Eden, C. P. Broeren, *J. Autoimmun.* **2005**, *25*, 172.
[41] R. van Eenige, P. S. Verhave, P. J. Koemans, I. A. C. W. Tiebosch, P. C. N. Rensen, S. Kooijman, *PLoS One* **2020**, *15*, 0237096.
[42] A. Hanyecz, S. E. Berlo, S. Szántó, C. P. M. Broeren, K. Mikecz, T. T. Glant, *Arthritis Rheum.* **2004**, *50*, 1665.
[43] L. Piemonti, P. Monti, P. Allavena, M. Sironi, L. Soldini, B. E. Leone, C. Socci, V. Di Carlo, *J. Immunol.* **1999**, *162*, 6473.
[44] D. Rozkova, R. Horvath, J. Bartunkova, R. Spisek, *Clin. Immunol.* **2006**, *120*, 260.
[45] E. R. Weikum, M. T. Knuesel, E. A. Ortlund, K. R. Yamamoto, *Nat. Rev. Mol. Cell Biol.* **2017**, *18*, 159.
[46] M. Kadmiel, J. A. Cidlowski, *Trends Pharmacol. Sci.* **2013**, *34*, 518.
[47] A. Wakkach, N. Fournier, V. Brun, J.-P. Breittmayer, F. Cottrez, H. Groux, *Immunity* **2003**, *18*, 605.
[48] M. K. Levings, R. Bacchetta, U. Schulz, M. G. Roncarolo, *Int. Arch. Allergy Immunol.* **2002**, *129*, 263.
[49] V. Rothhammer, F. J. Quintana, *Nat. Rev. Immunol.* **2019**, *19*, 184.
[50] A. L. Mellor, D. H. Munn, *Nat. Rev. Immunol.* **2004**, *4*, 762.
[51] S. G. Jeon, H. Kayama, Y. Ueda, T. Takahashi, T. Asahara, H. Tsuji, N. M. Tsuji, H. Kiyono, J. S. Ma, T. Kusu, R. Okumura, H. Hara, H. Yoshida, M. Yamamoto, K. Nomoto, K. Takeda, *PLoS Pathog.* **2012**, *8*, 1002714.
[52] T. Volz, Y. Skabytska, E. Guenova, K.-M. Chen, J.-S. Frick, C. J. Kirschning, S. Kaesler, M. Röcken, T. Biedermann, *J. Invest. Dermatol.* **2014**, *134*, 96.
[53] G. Nocentini, L. Giunchi, S. Ronchetti, L. T. Krausz, A. Bartoli, R. Moraca, G. Migliorati, C. Riccardi, *Proc. Natl. Acad. Sci. USA* **1997**, *94*, 6216.
[54] Y. Carrier, M. J. Whitters, J. S. Miyashiro, T. P. LaBranche, H. E. Ramon, S. E. Benoit, M. S. Ryan, S. P. Keegan, H. Guay, J. Douhan, M. Collins, K. Dunussi-Joannopoulos, Q. G. Medley, *Eur. J. Immunol.* **2012**, *42*, 1393.
[55] A. E. Anderson, D. J. Swan, O. Y. Wong, M. Buck, O. Eltherington, R. A. Harry, A. M. Patterson, A. G. Pratt, G. Reynolds, J.-P. Doran, J. A. Kirby, J. D. Isaacs, C. M. U. Hilkens, *Clin. Exp. Immunol.* **2017**, *187*, 113.
[56] T. L. Nguyen, Y. Choi, J. Im, H. Shin, N. M. Phan, M. K. Kim, S. W. Choi, J. Kim, *Nat. Commun.* **2022**, *13*, 7449.
[57] J. D. Whalen, E. L. Lechman, C. A. Carlos, K. Weiss, I. Kovesdi, J. C. Glorioso, P. D. Robbins, C. H. Evans, *J. Immunol.* **1999**, *162*, 3625.
[58] A. Finnegan, C. D. Kaplan, Y. Cao, *Arthritis Res. Ther.* **2003**, *5*, R18.
[59] S. Mitragotri, J. W. Yoo, *Arch. Pharmacal. Res.* **2011**, *34*, 1887.
[60] M. Lorscheider, N. Tsapis, M. ur-Rehman, F. Gaudin, I. Stolfa, S. Abreu, S. Mura, P. Chaminade, M. Espeli, E. Fattal, *J. Controlled Release* **2019**, *296*, 179.
[61] R. R. Meka, S. H. Venkatesha, B. Acharya, K. D. Moudgil, *Nanomedicine* **2019**, *14*, 1455.
[62] F. Yan, Z. Zhong, Y. Wang, Y. Feng, Z. Mei, H. Li, X. Chen, L. Cai, C. Li, *J. Nanobiotechnol.* **2020**, *18*, 115.
[63] N. R. H. Stone, T. Bicanic, R. Salim, W. Hope, *Drugs* **2016**, *76*, 485.
[64] World Health Organ Model List of Essential Medicines. World Health Organ. **2023**.
[65] M. J. Mansilla, C. M. U. Hilkens, E. M. Martínez-Cáceres, *Immunother. Adv.* **2023**, *3*, itad012.
[66] A. Sonigra, H. J. Nel, P. Wehr, N. Ramnoruth, S. Patel, K. A. van Schie, M. W. Bladen, A. M. Mehdi, J. Tesiram, M. Talekar, J. Rossjohn, H. H. Reid, F. E. Stuurman, H. Roberts, P. Vecchio, I. Gourley, M. Rigby, S. Becart, R. E. M. Toes, H. U. Scherer, K.-A. Lê Cao, K. Campbell, R. Thomas, *JCI Insight* **2022**, *7*, e160964.